

ELECTRONIC SUPPLEMENTARY INFORMATION

Effect of Cholesterol on Membrane Partitioning Dynamics of Hepatitis A Virus-2B peptide

Samapan Sikdar ^{1,2}, Manidipa Banerjee ³ and Satyavani Vemparala ^{1,2}

¹ The Institute of Mathematical Sciences, C.I.T. Campus, Taramani, Chennai 600113, India

² Homi Bhabha National Institute, Training School Complex, Anushakti Nagar, Mumbai, 400094, India

³ Kusuma School of Biological Sciences, Indian Institute of Technology-Delhi, Hauz Khas, New Delhi -110016, India.

Corresponding authors:

Email: samapans@imsc.res.in; mbanerjee@bioschool.iitd.ac.in; vani@imsc.res.in

<i>Systems</i>	System size	n_w	Simulation time (ns)	Equilibration time (ns)
<i>HAV-2B – Water</i>	22288	–	400	100
<i>Pure POPC</i>	70306	35	350	150
<i>Mixed POPC – Chol(20%)</i>	66710	35	350	150
<i>Mixed POPC – Chol(40%)</i>	63232	35	350	150
<i>HAV-2B – POPC Replica 1</i>	104280	72	500	300
<i>HAV-2B – POPC - Chol(20%) Replica 1</i>	93379	64	715	450
<i>HAV-2B – POPC Replica 2</i>	105356	74	415	200
<i>HAV-2B – POPC - Chol(20%) Replica 2</i>	99874	71	435	200

Table S1. Details of systems considered in the present study. All atom MD simulations of HAV-2B peptide are performed in different media: Water, hydrated POPC bilayer and hydrated POPC-Chol(20%) bilayer. Pure POPC, Mixed POPC-Chol(20%) and POPC-Chol(40%) refers to control membrane systems in absence of the peptide. The system size denoted by total number of atoms; number of water molecules per lipid, n_w followed by the simulation time and the equilibration time for each system are provided as well.

<i>Residue id</i>	<i>HAV-2B - POPC</i>	<i>HAV-2B – POPC- Chol(20%)</i>	<i>Residue id</i>	<i>HAV-2B - POPC</i>	<i>HAV-2B – POPC- Chol(20%)</i>	<i>Residue id</i>	<i>HAV-2B - POPC</i>	<i>HAV-2B – POPC- Chol(20%)</i>
V1	36.9	0	V21	100.0	0	N41	100.0	13.4
T2	11.4	0	I22	100.0	0	Y42	100.0	12.5
V3	0	0	Q23	100.0	0	A43	100.0	0
E4	0	0	Q24	100.0	0	D44	94.5	2.6
I5	0	0	L25	100.0	0	I45	100.0	0
I6	0	0	N26	100.0	0	G46	97.2	0.9
N7	0	0	Q27	100.0	0	C47	100.0	2.6
T8	0	0	D28	99.2	0	S48	100.0	53.5
V9	0.4	0	E29	62.3	0	V49	100.0	58.7
L10	8.6	0	H30	83.5	0	I50	100.0	100.0
C11	7.8	0.29	S31	49.4	0	S51	100.0	91.3
F12	91.0	7.8	H32	89.8	0	C52	94.5	24.1
V13	32.2	1.4	I33	100.0	0	G53	100.0	41.9
K14	93.7	46.2	I34	97.6	0.6	K54	100.0	79.6
S15	100.0	54.9	G35	100.0	0	V55	100.0	13.7
G16	100.0	9.3	L36	100.0	0	F56	100.0	5.8
I17	100.0	1.4	L37	100.0	0	S57	100.0	10.2
L18	100.0	0	R38	99.2	6.7	K58	99.2	1.2
L19	100.0	0	V39	100.0	0	M59	100.0	1.2
Y20	100.0	0	M40	100.0	0	L60	100.0	1.2

Table S2. Contact probability of HAV-2B peptide residues with membrane computed over last 50 ns of equilibrated trajectories. The residues showing contact probability > 75% are highlighted in colour according to its nature: Hydrophobic (Green) and Hydrophilic (magenta).

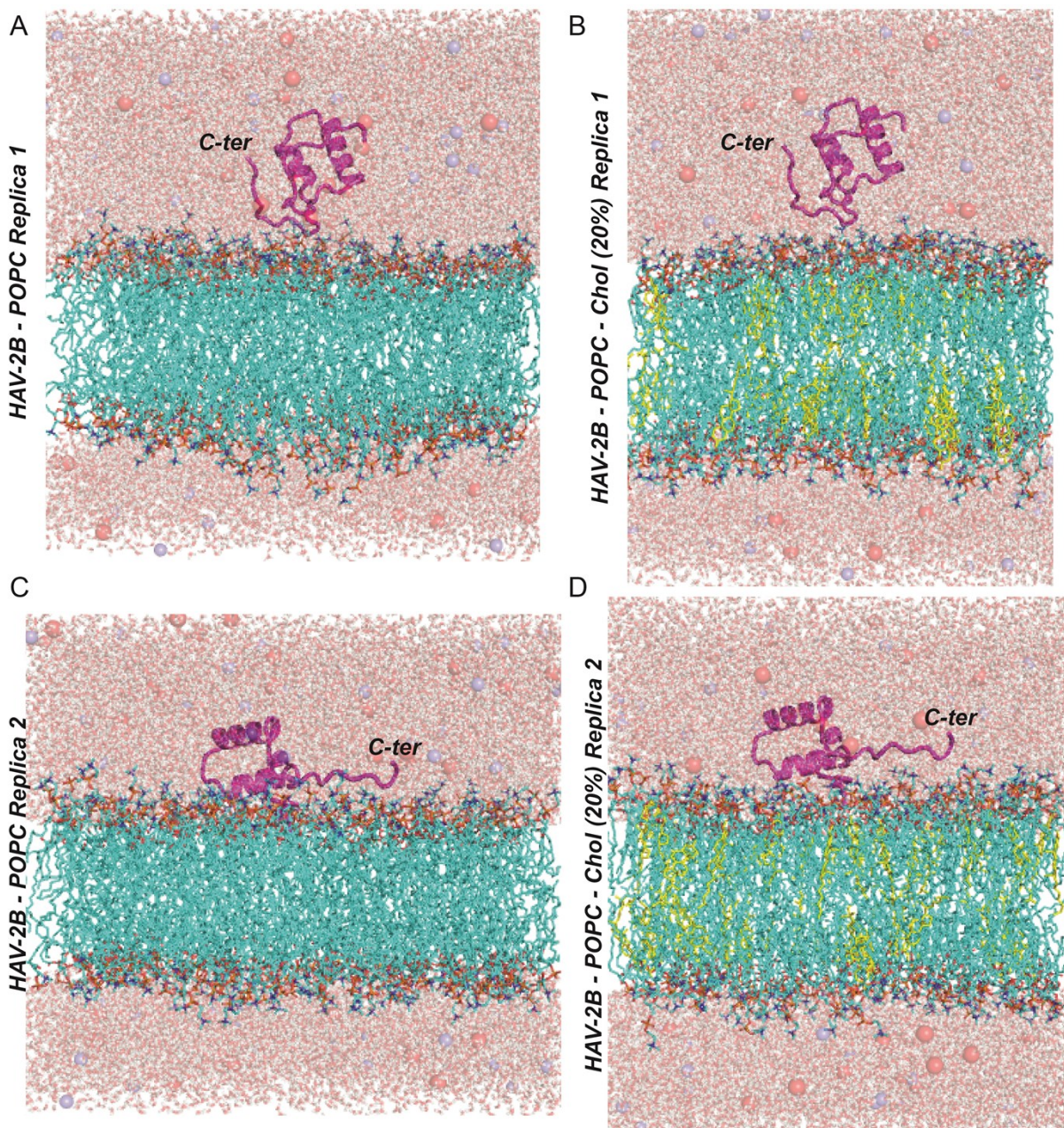


Fig S1. The initial snapshots of HAV-2B peptide-membrane systems considered in this study. A compact conformation of peptide, with α -helical hairpin motif oriented parallel to membrane normal is considered in Replica 1 simulations, while an extended peptide conformation with the hairpin motif placed parallel to bilayer surface is considered as Replica 2. The HAV-2B peptide (magenta), POPC (cyan), cholesterol (yellow), water, sodium (red) and chlorine (blue) ions are shown.

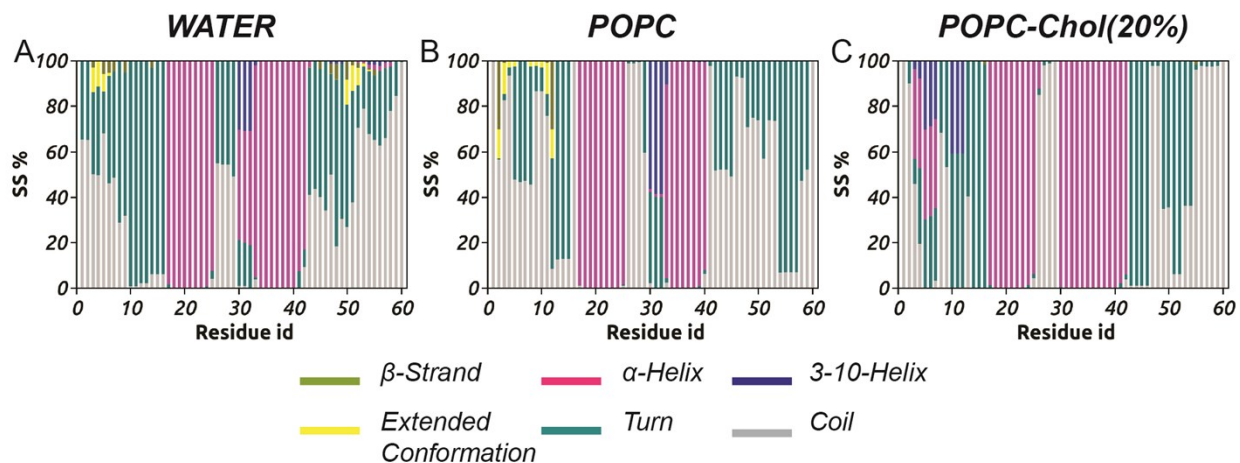


Fig S2. Residue based secondary structure (SS) % of HAV-2B peptide in (A) water, (B) in POPC and (C) in POPC-Chol(20%) bilayers, showing population of different secondary structural elements accessible to each residue.

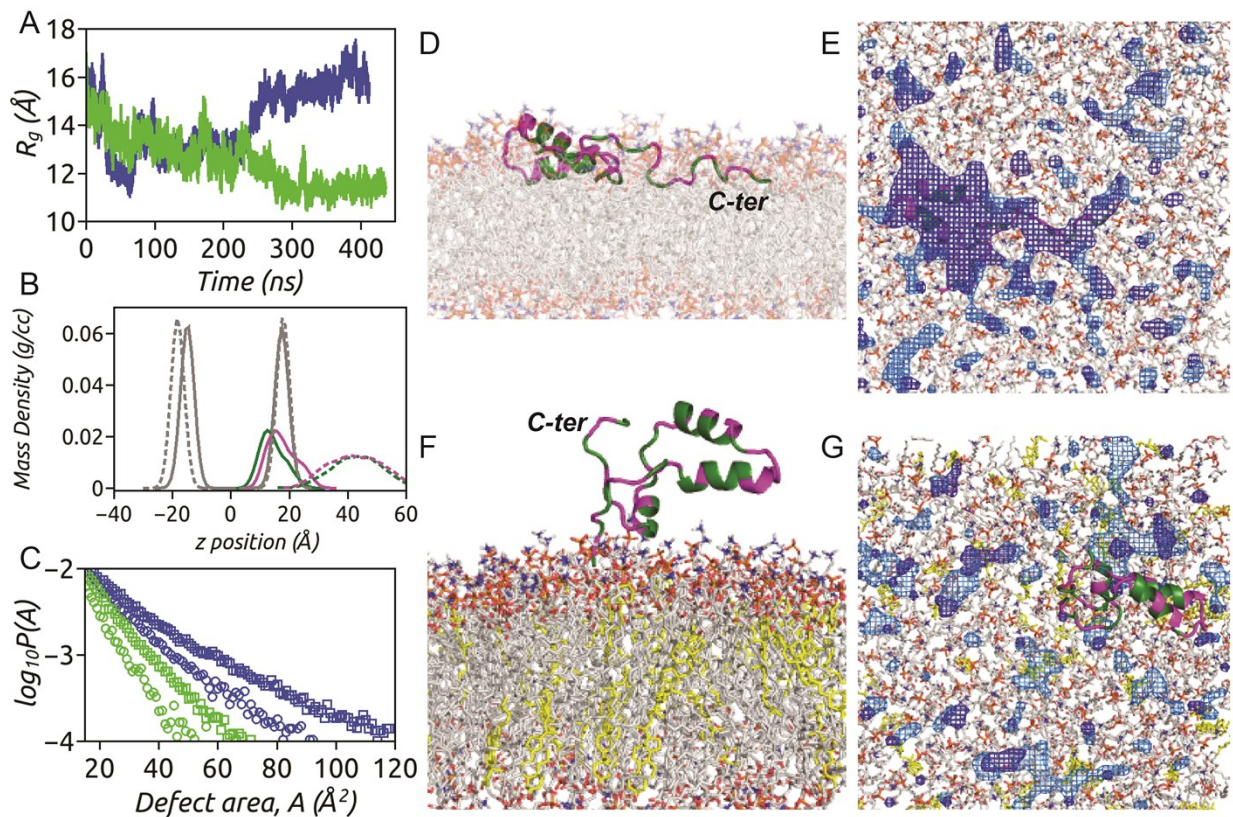


Fig S3. **The results of Replica 2 simulations are illustrated.** (A) The time evolution of R_g of HAV-2B peptide in POPC (blue) and POPC-Chol(20%) (green) bilayers. (B) The mass density profiles along the bilayer normal (z -direction) are indicated for HAV-2B peptide in POPC (solid lines) and POPC-Chol(20%) (dotted lines) bilayers. The hydrophobic (green) and hydrophilic (magenta) density profiles of the peptide segregate towards bilayer centre and lipid headgroups (gray), respectively, in absence of cholesterol, indicating peptide partitioning. However peptide insertion is not observed in POPC-Chol (20%) bilayer and these densities are overlapping and located in bulk solvent. (C) The size distribution, $\log_{10} P(A)$ of “Deep” (circle) and “Shallow” (square) defects in POPC (blue) and POPC-Chol(20%) (green) bilayers in presence of HAV-2B peptide. The peptide partitioning significantly enhances both number and size of defect sites in cholesterol free POPC bilayer. Representative snapshots illustrating peptide-membrane binding mode in Replica 2 simulations are shown in (D)-(G). The side- (D) and top- (E) view of peptide partitioning into POPC bilayer facilitated by a large co-localized “Deep” defect. The side- (F) and top- (G) view of peptide close to POPC-Chol(20%) bilayer. The hydrophobic and hydrophilic residues are coloured in green and magenta, respectively, lipid tails in gray and cholesterol in yellow. The “Deep” (dark blue) and “Shallow” (light blue) defects are shown in mesh representation.

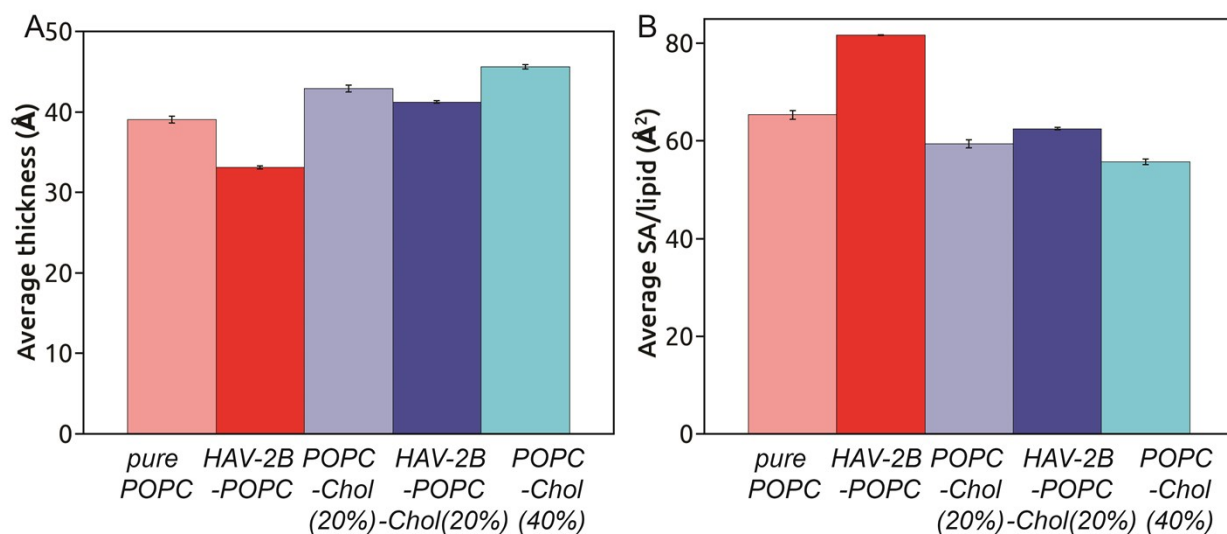


Fig S4. (A) Average bilayer thickness and (B) average surface area (SA) per lipid for different systems, computed over equilibrated trajectories.

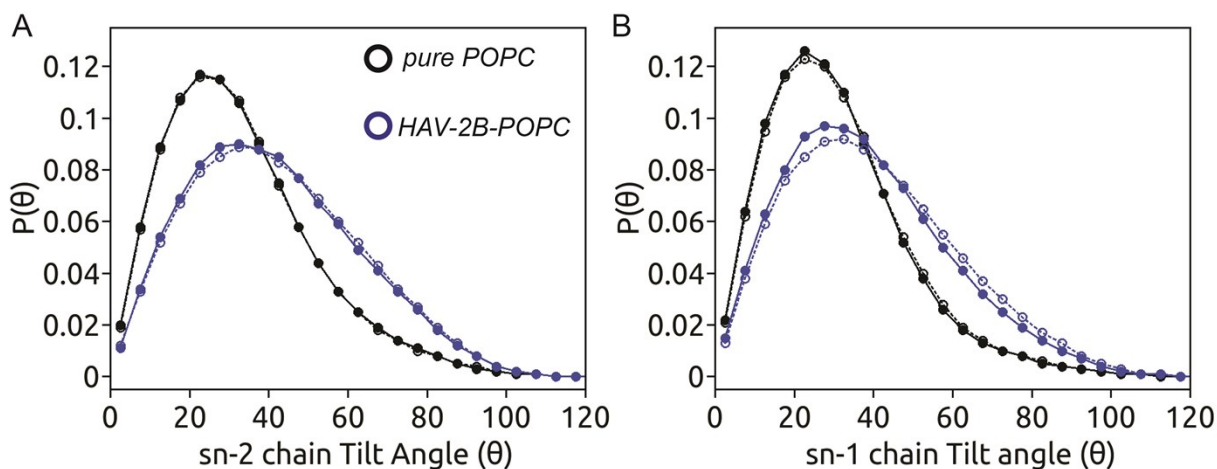


Fig S5. The distribution of lipid tail tilt angles for (A) $sn-2$ and (B) $sn-1$ chains in control pure POPC (black) and HAV-2B-POPC (blue) bilayers. The values for top leaflet are shown in solid symbol and solid line, while that of bottom leaflet are shown in open symbol and dotted line.

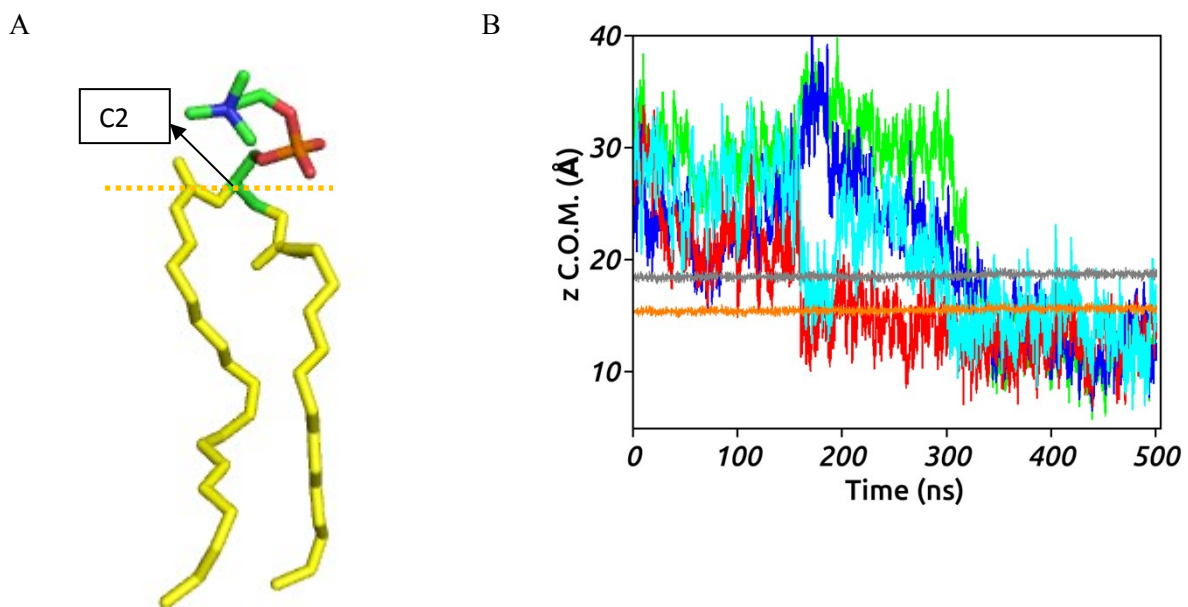


Fig S6 (A). C2 atom of glycerol moiety of POPC molecule based on the level of which defects are classified as “Deep” or “Shallow”. (B) The insertion dynamics of M40 (green), Y42 (blue), F56 (red) and M59 (cyan) residues from C-terminal tail of HAV-2B peptide, which show maximum insertion depth in

POPC bilayer. The average levels of POPC haedgroup atoms, P (grey) and glycerol, C2 (orange) are shown. Insertion of F56 occurs at 160 ns and remains embedded below the C2 level for rest of the time.

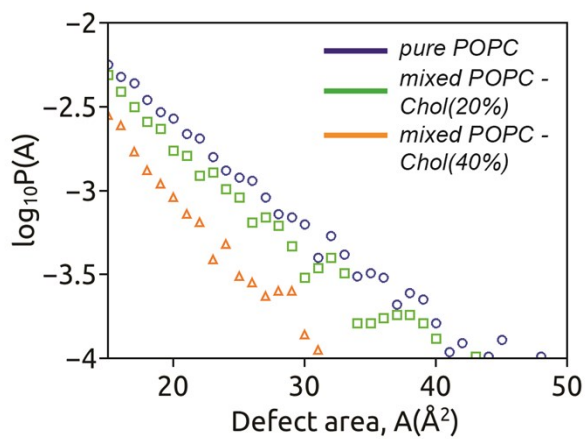


Fig S7. The size distribution of “Deep” defects found in the control systems: pure POPC (blue), mixed POPC-Chol(20%) (green) and POPC-Chol(40%) (orange).

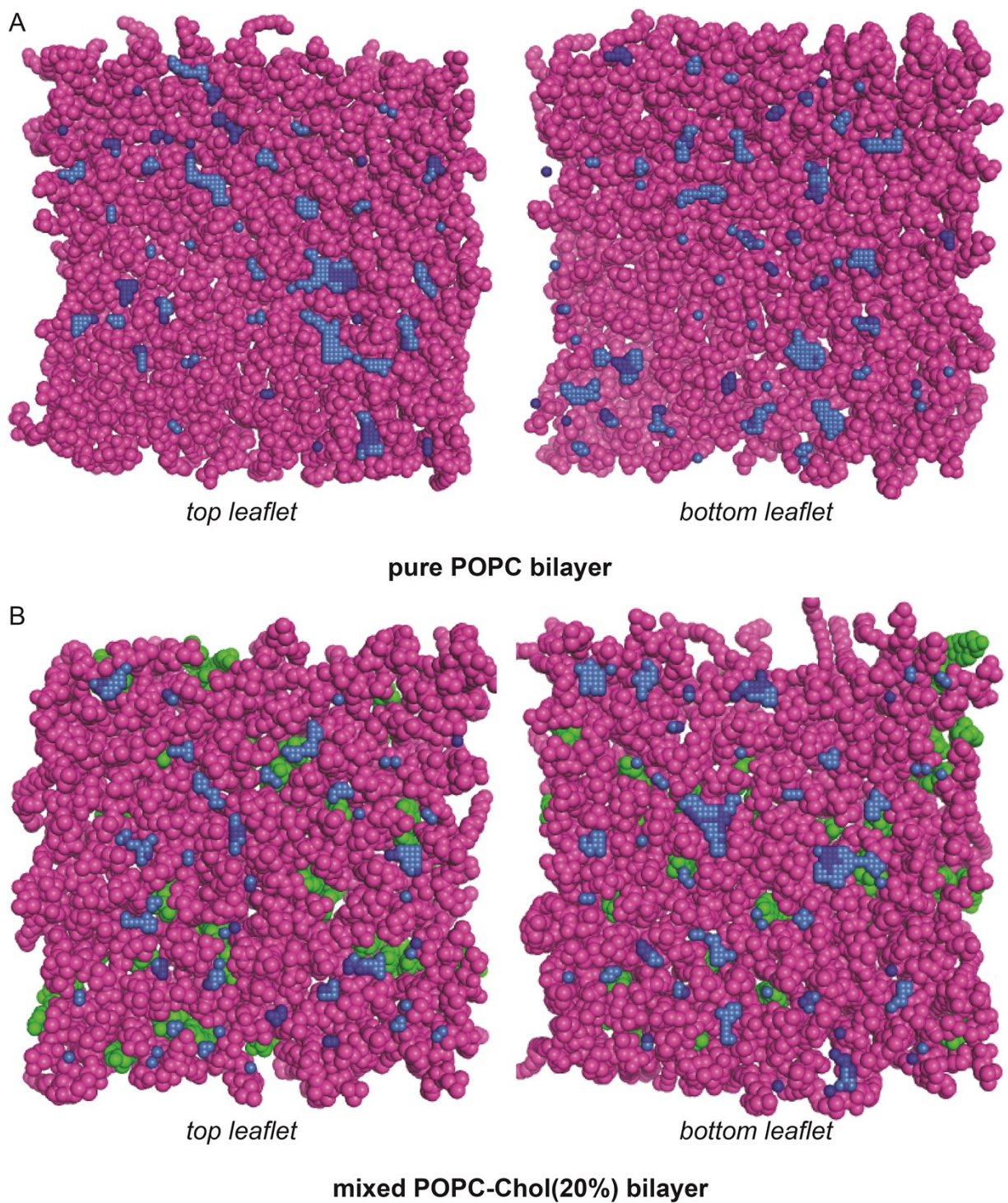


Fig S8. Representative snapshots of final MD structures showing packing defects in each leaflet of the control systems. POPC (magenta) and cholesterol (green) along with superposed “Deep” (dark blue) and “Shallow” (light blue) lipid packing defects are shown.

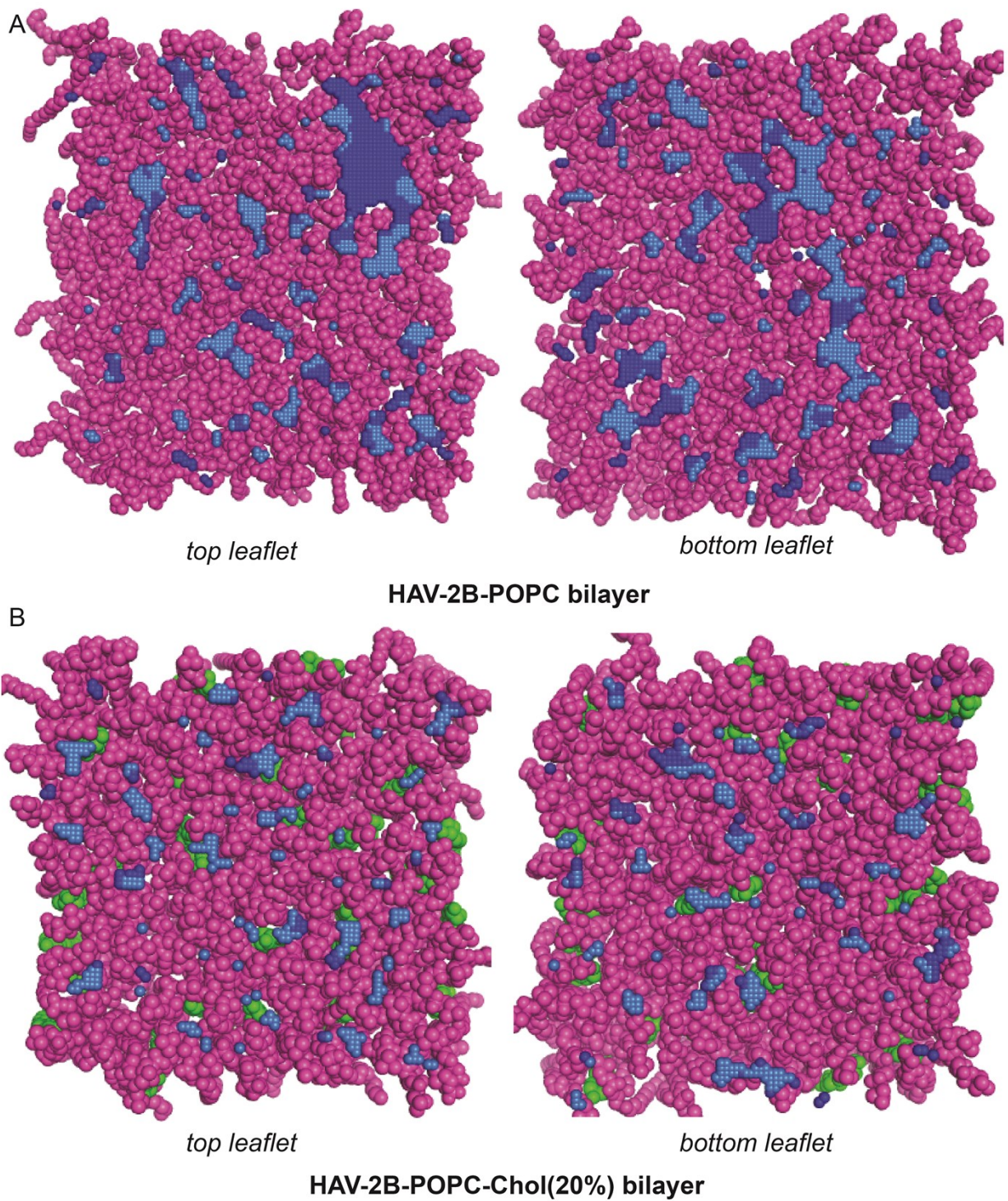


Fig S9. Representative snapshots of final MD structures showing packing defects in each leaflet of the peptide-membrane systems. POPC (magenta) and cholesterol (green) along with superposed “Deep” (dark blue) and “Shallow” (light blue) lipid packing defects are shown.

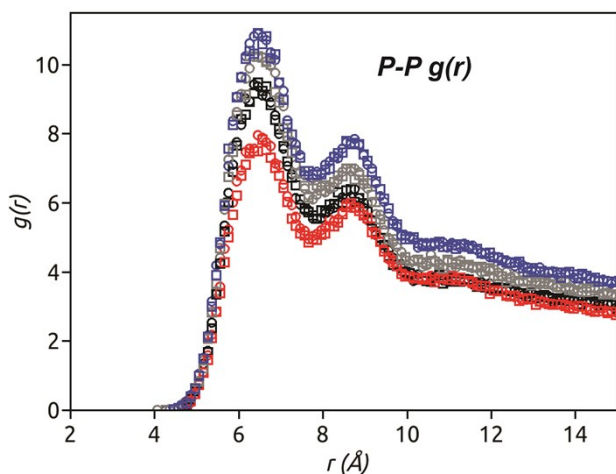


Fig S10. Radial distribution function, $g(r)$ of POPC headgroups considering phosphate (P) atoms of top (circle) and bottom (square) leaflets of different systems: pure POPC (black) and in presence of HAV-2B peptide (red), mixed POPC-Cholesterol (20%) (gray) and in presence of peptide (blue).

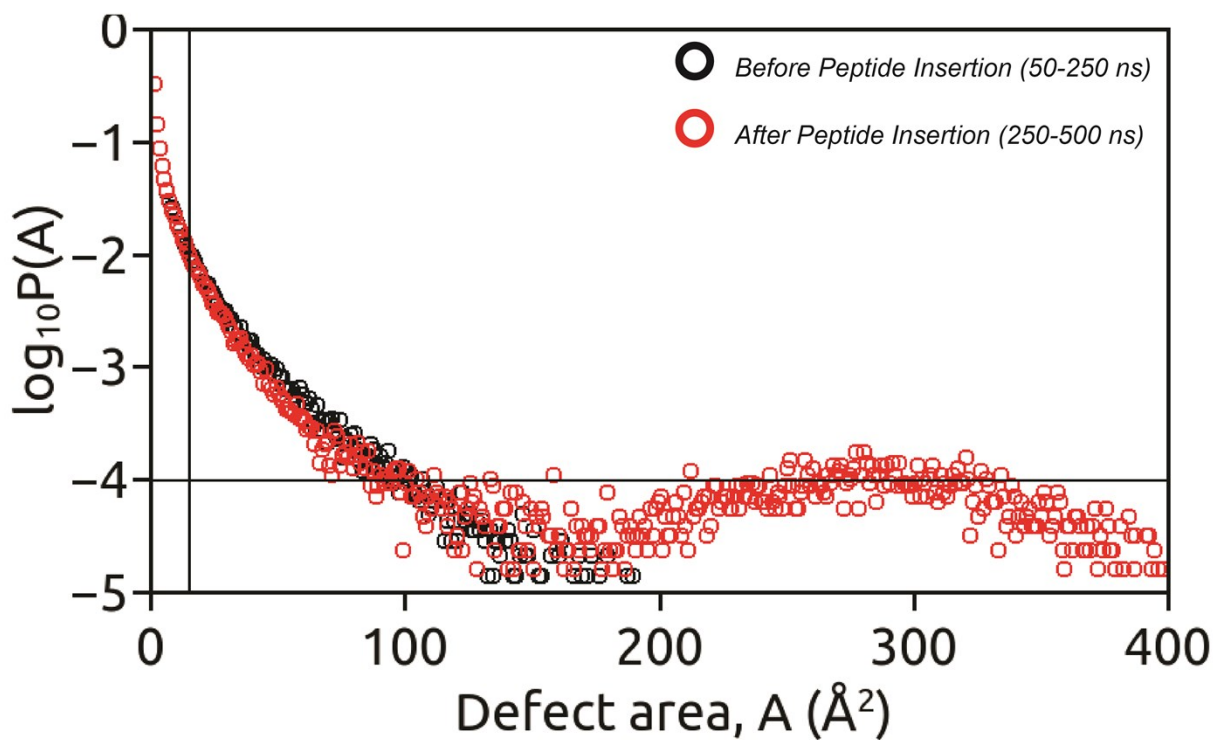


Fig S11. The effect of HAV-2B peptide partitioning on the probability distributions of defect sizes (in \AA^2), computed separately for 50-250 ns (before peptide insertion) and 250-500 ns (after peptide insertion).

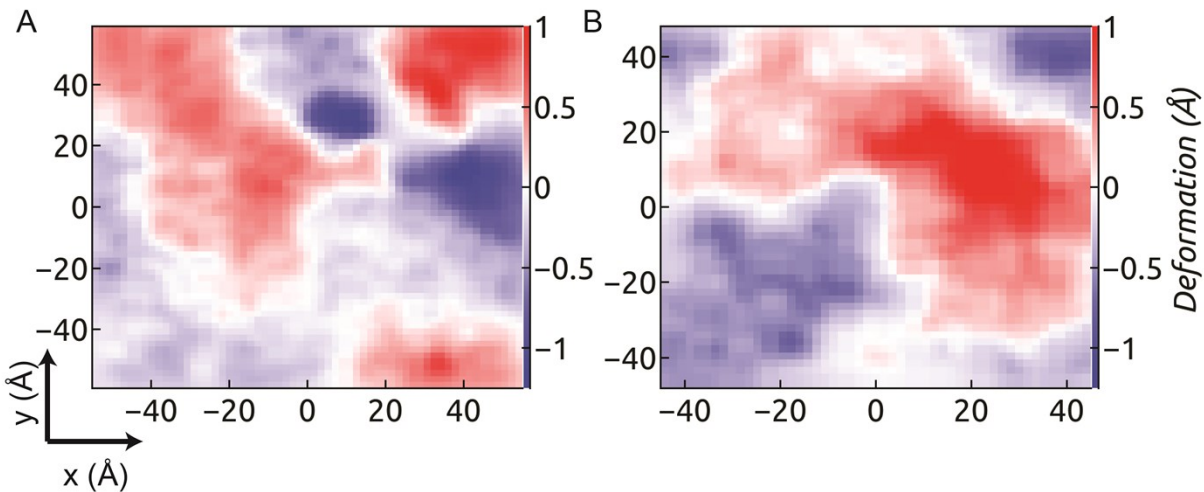


Fig S12. The 2d-maps represent leaflet deformation calculated as the distance of each phosphate (P) atom from the average phosphate level along z-direction in a given leaflet, generated using a 2Å resolution along each direction, averaged over the last 50 ns trajectories of HAV-2B peptide in (A) POPC and (B) POPC-Chol(20%) bilayers. A negative value of deformation indicates inward bending and vice-versa. The leaflet deformation is more pronounced in (A) compared to (B) indicating inward bending around the HAV-2B peptide insertion site.